OMTM, Volume *6*

Supplemental Information

A Five-Repeat Micro-Dystrophin Gene Ameliorated Dystrophic Phenotype in the Severe DBA/2J-mdx Model of Duchenne Muscular Dystrophy

Chady H. Hakim, Nalinda B. Wasala, Xiufang Pan, Kasun Kodippili, Yongping Yue, Keqing Zhang, Gang Yao, Brittney Haffner, Sean X. Duan, Julian Ramos, Joel S. Schneider, N. Nora Yang, Jeffrey S. Chamberlain, and Dongsheng Duan

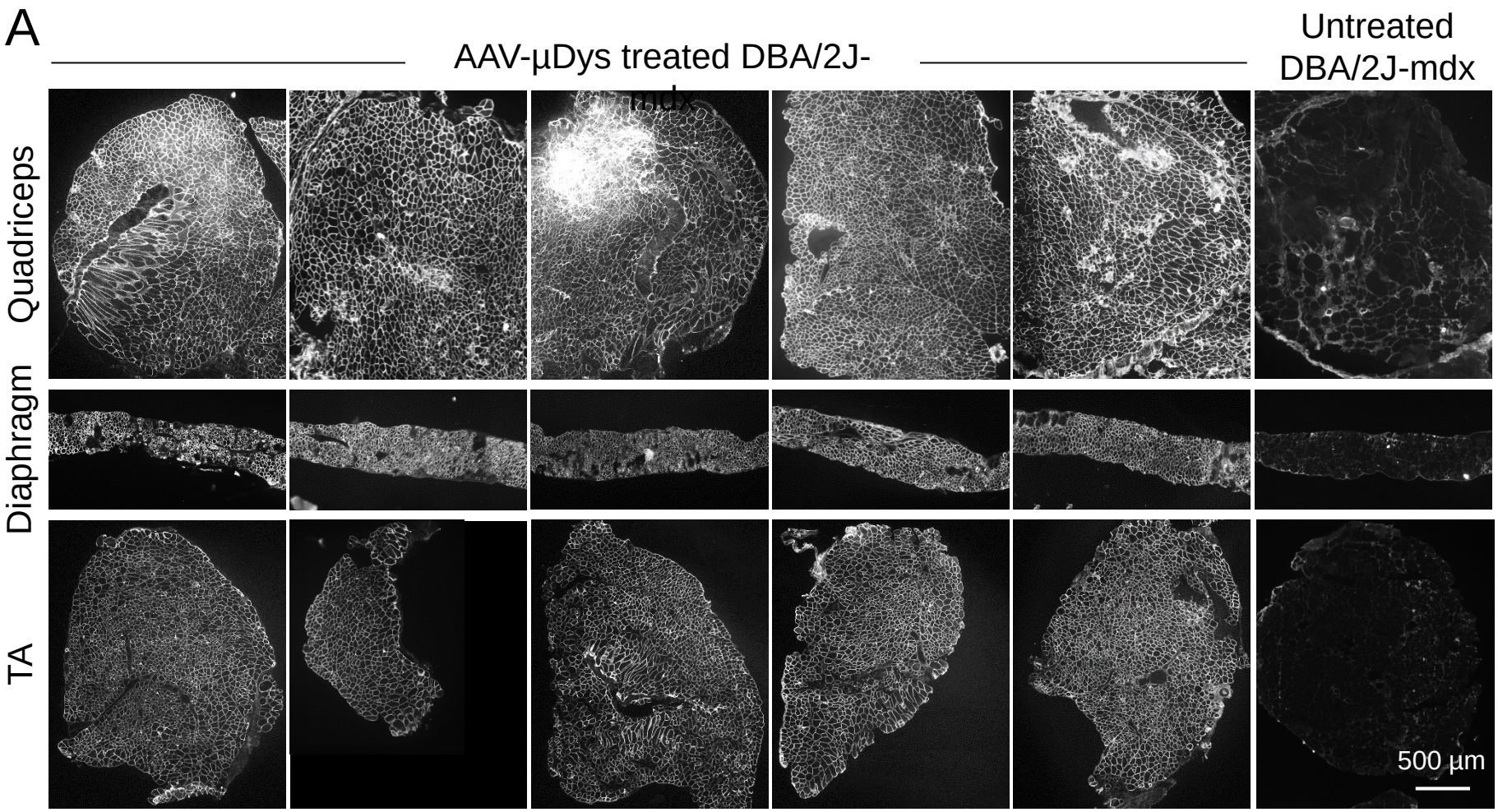
A
AAV-µDys treated DBA/2J-mdx
Untreated DBA/2J-mdx
Quadriceps
Diaphragm
TA
500 µm

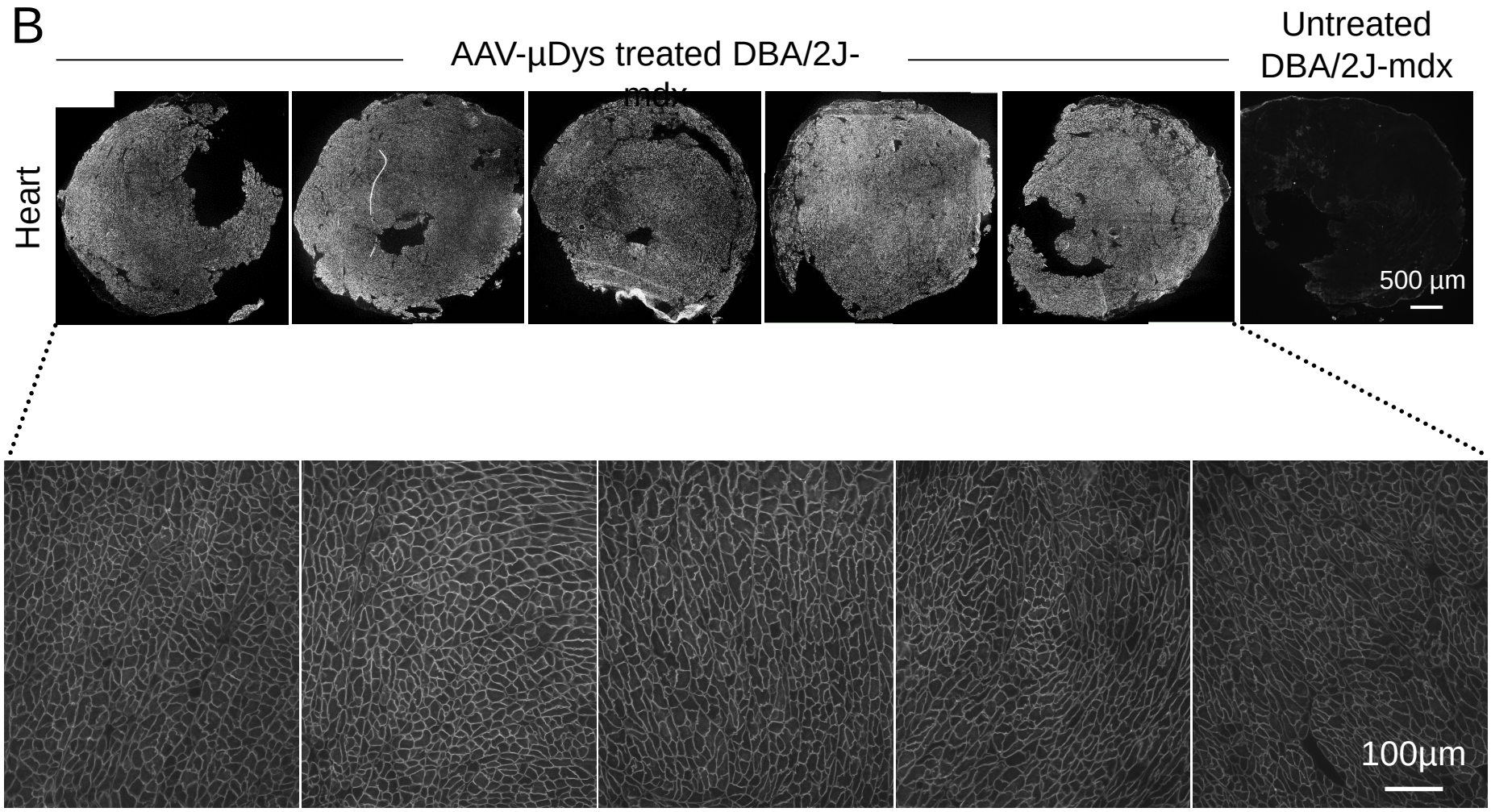
B
AAV-µDys treated DBA/2J-mdx
Untreated DBA/2J-mdx
Heart
500 µm
100µm

Hakim et al. 2017 Figure S1C

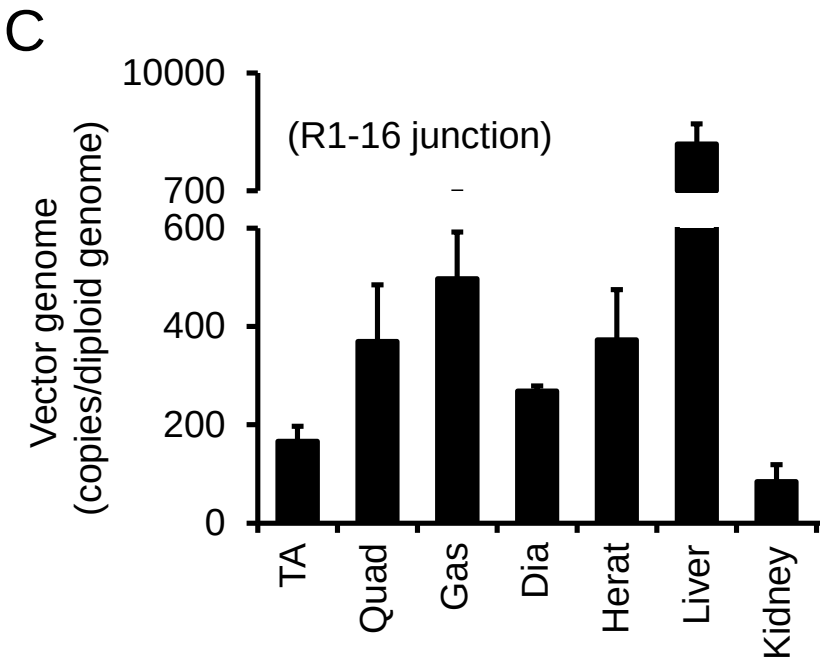

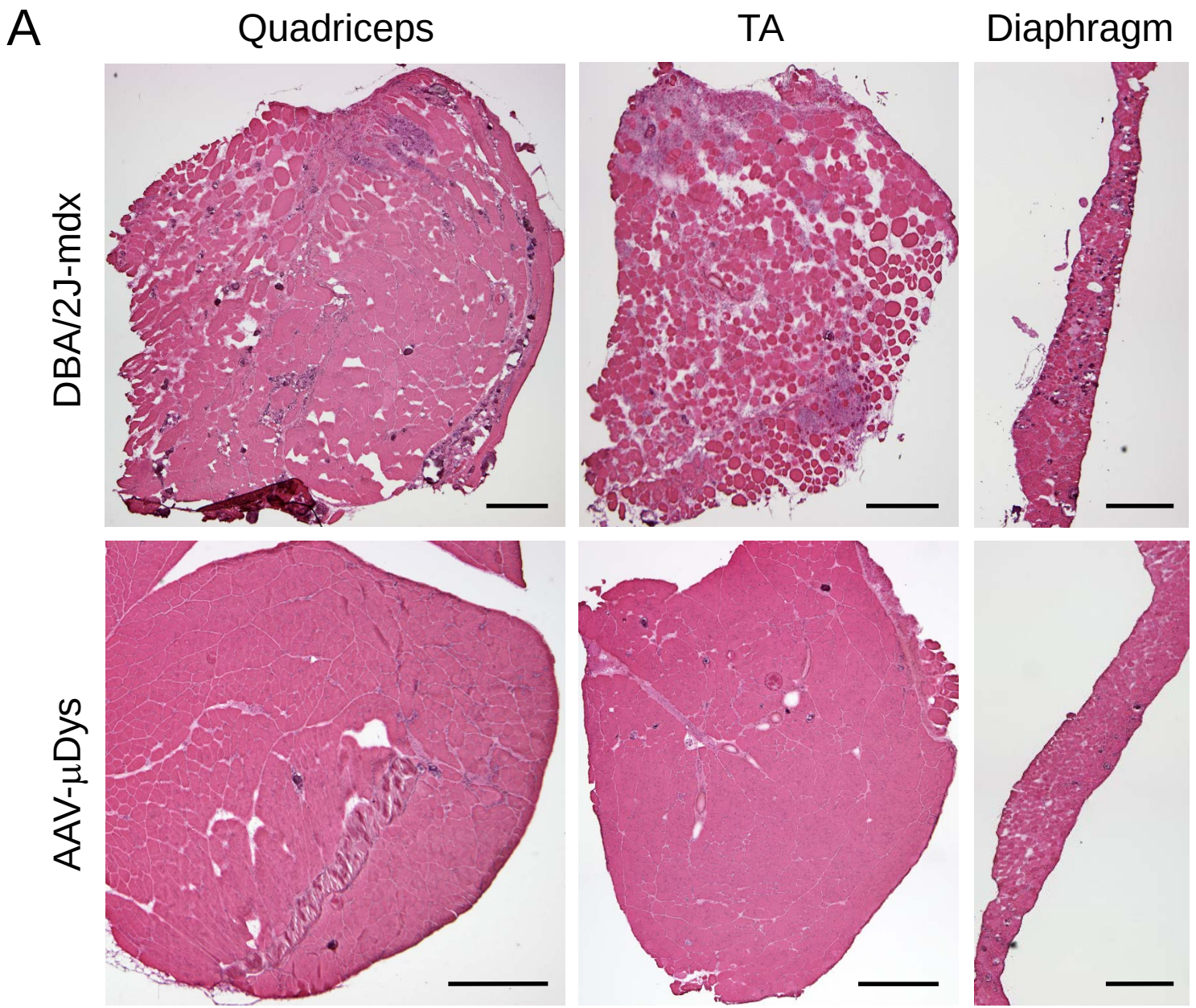
A
Quadriceps
TA
Diaphragm
DBA/2J-mdx
AAV-μDys

Hakim et al. 2017 Figure S2B

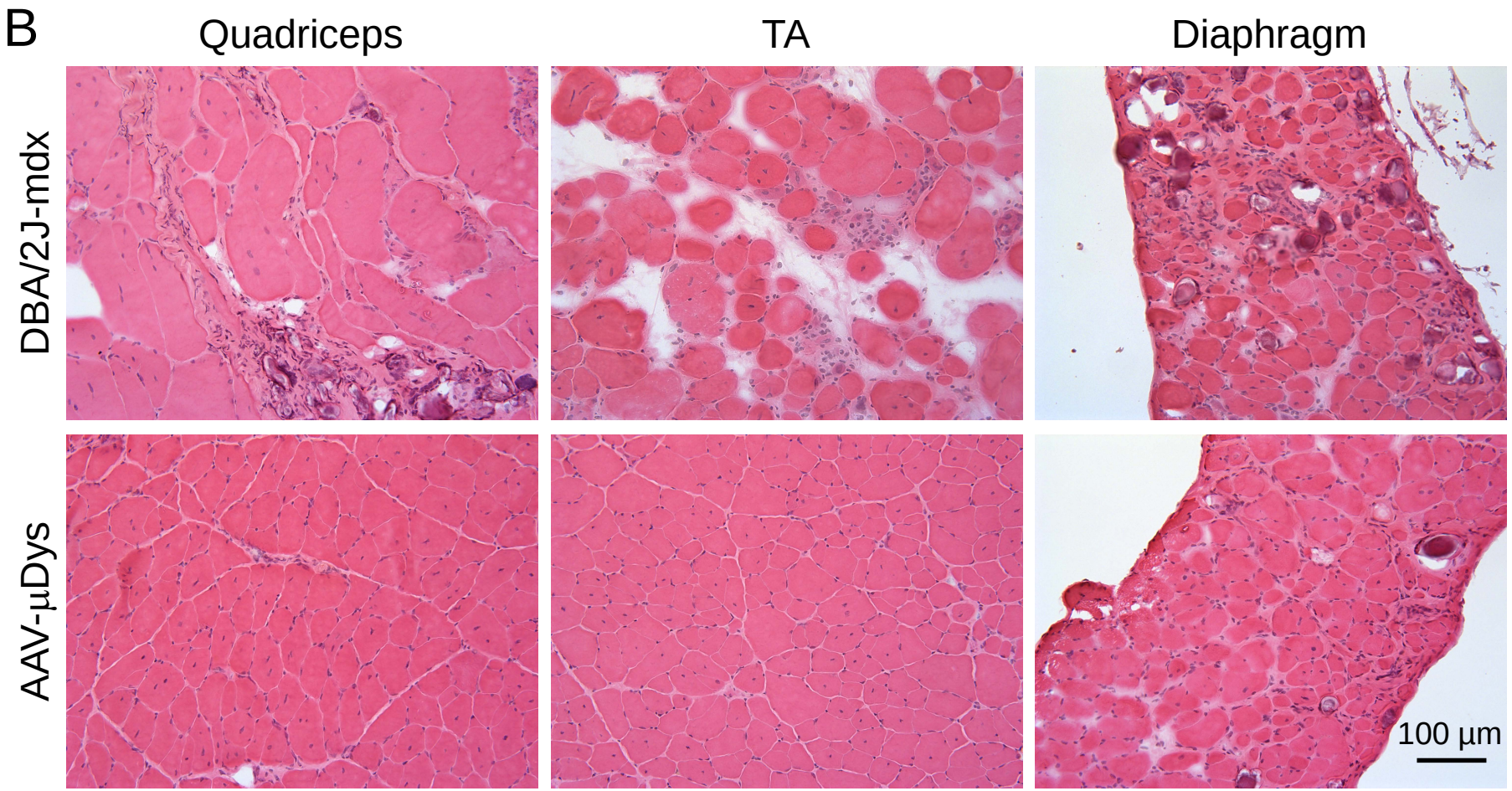

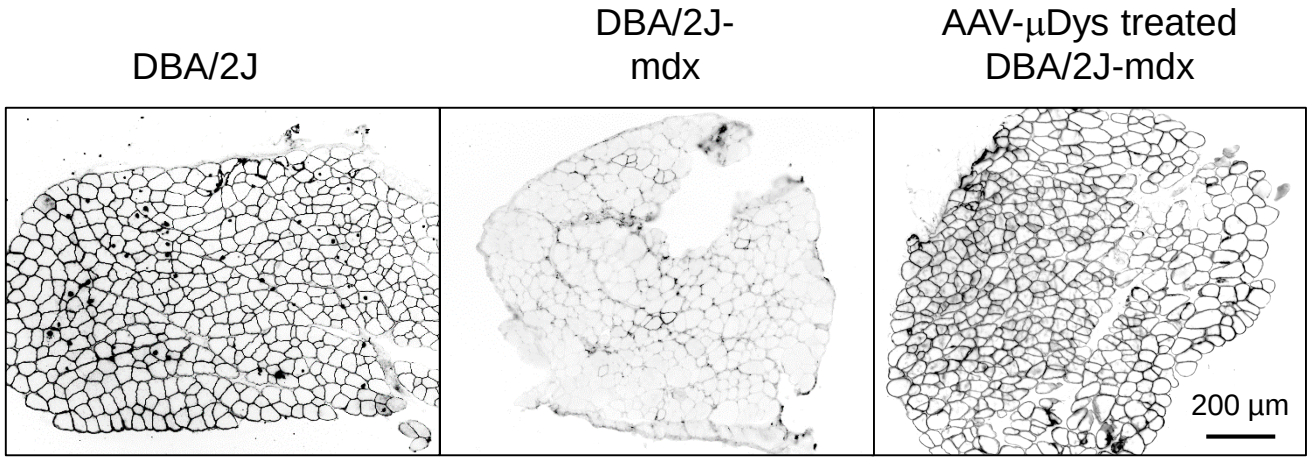
DBA/2J
DBA/2J-mdx
AAV-μDys treated DBA/2J-mdx
200 μm

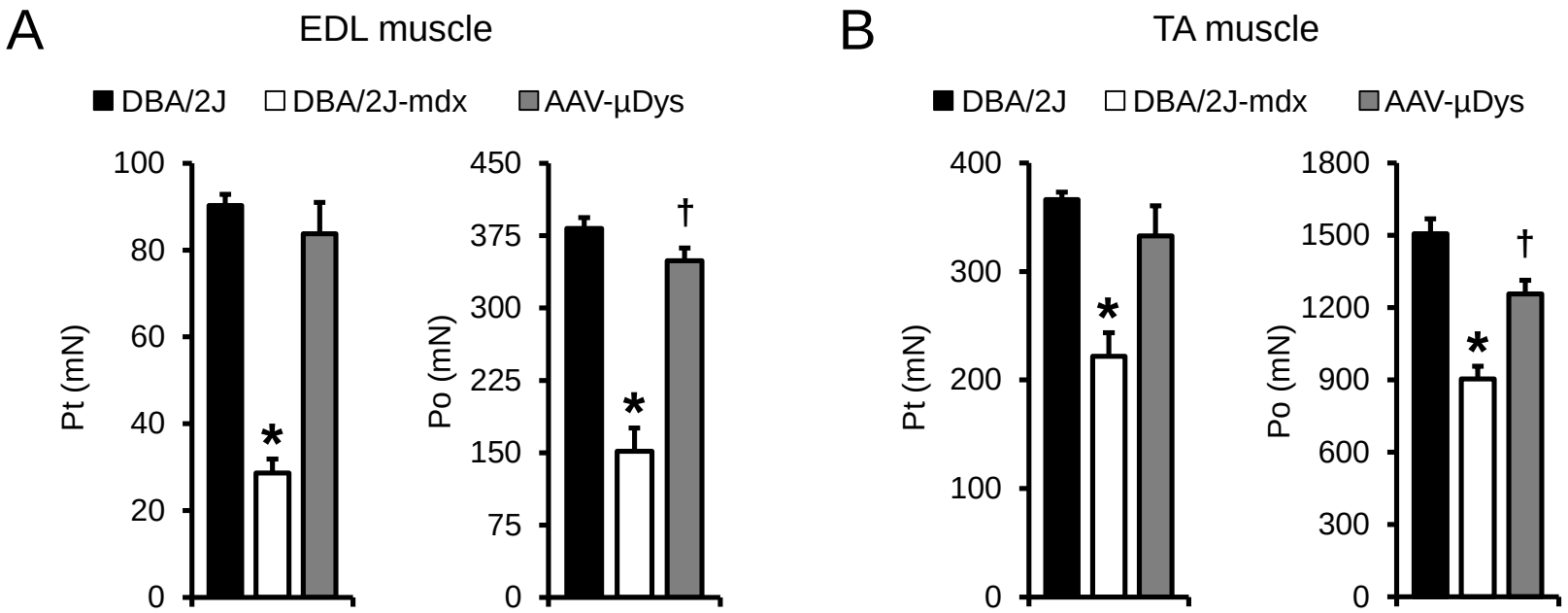

*, DBA/mdx is significant different from DBA and AAV treated
†, DBA is significant different from treated AAV treated

Hakim et al. 2017 Figure S5

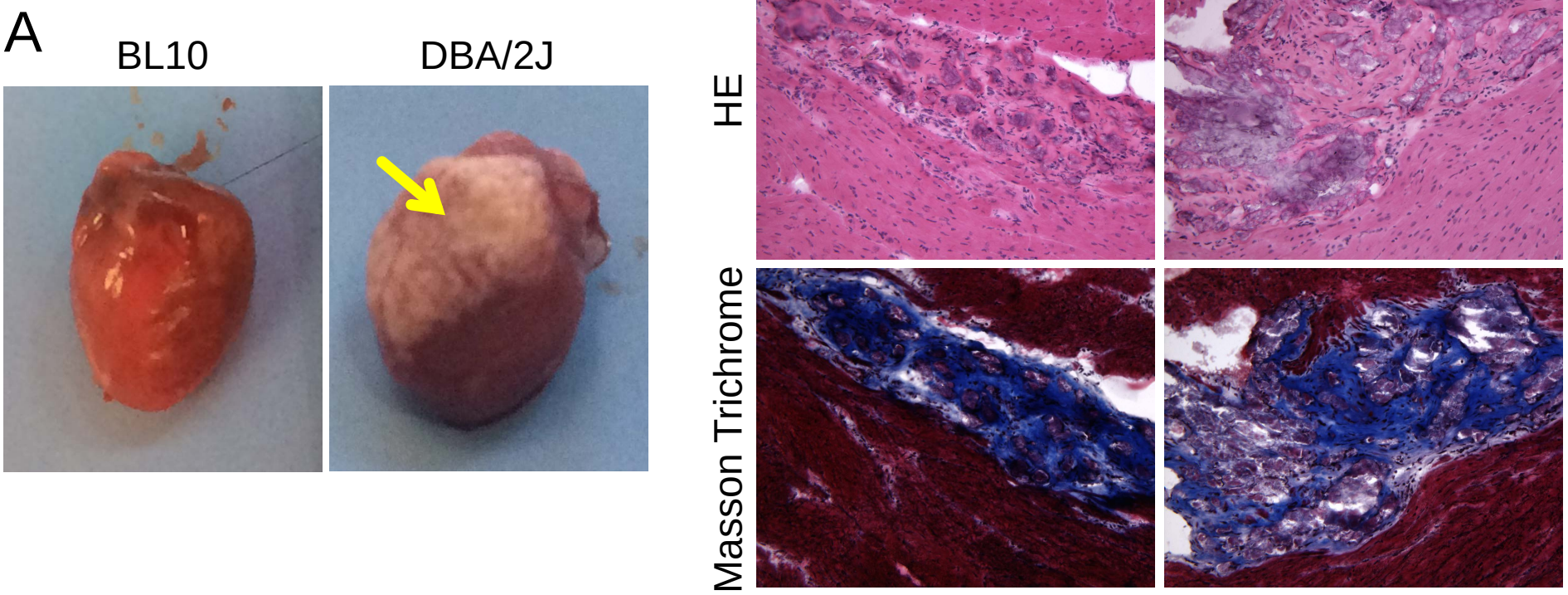

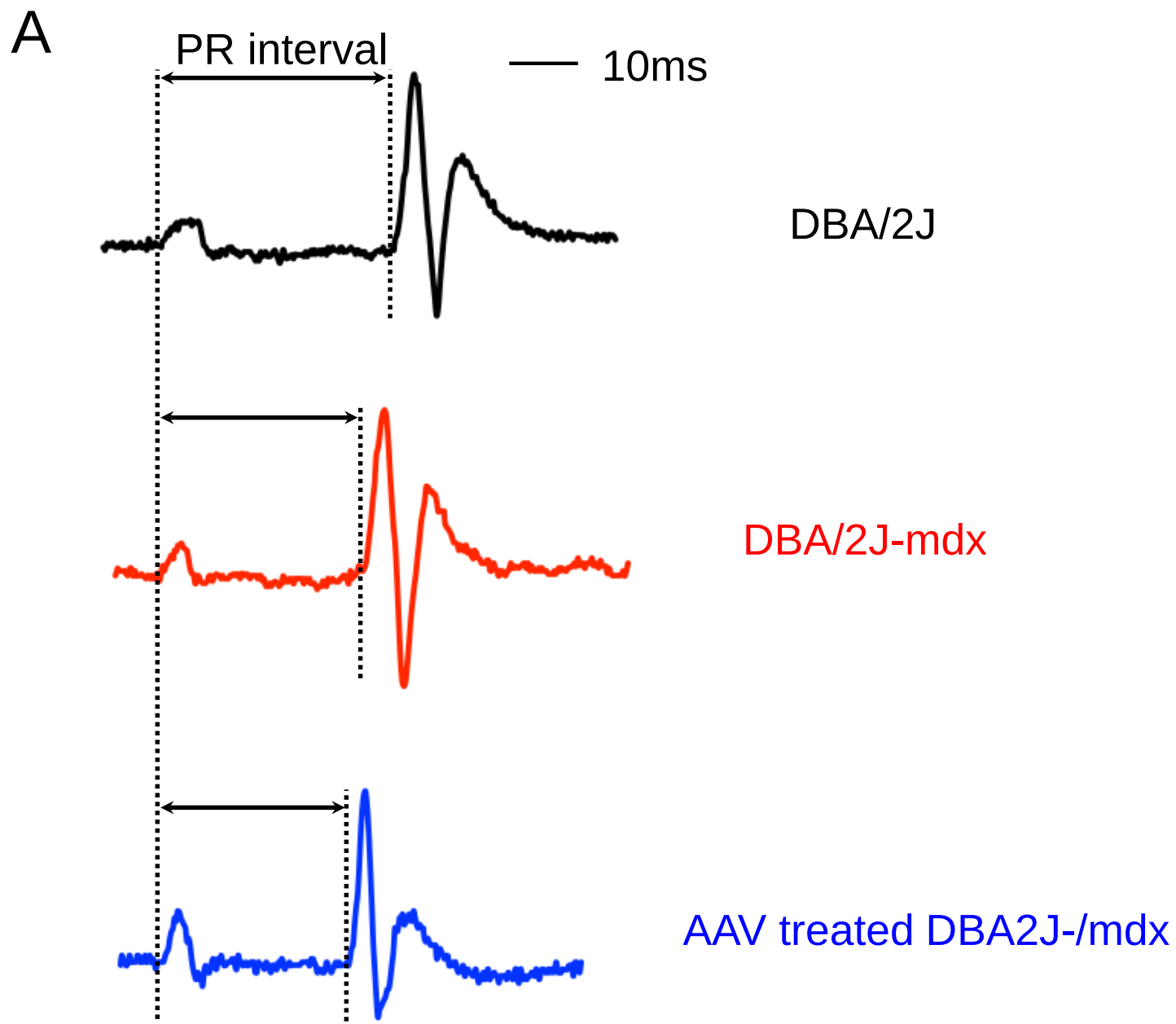
A
PR interval
10ms
DBA/2J
DBA/2J-mdx
AAV treated DBA2J-/mdx

Hakim et al. 2017 Figure S6B

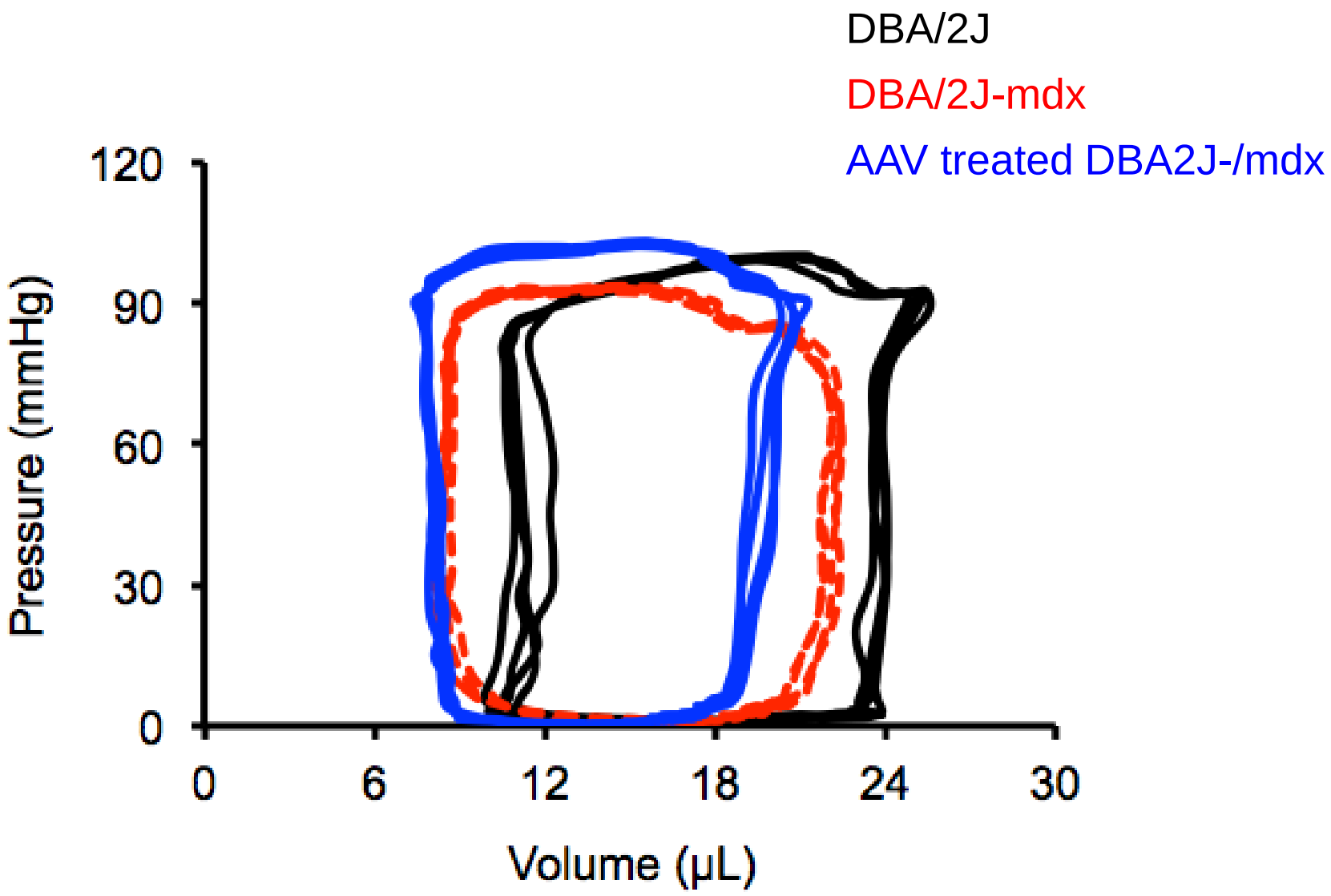

Supplemental Figure Legends

Figure S1. Widespread micro-dystrophin expression in skeletal muscle and the heart of AAV-9 treated DBA/2J-mdx mice. A, Representative photomicrographs of dystrophin immunostaining of the tibialis anterior muscle (TA), quadriceps and diaphragm from five AAV injected mice and an untreated DBA/2J-mdx mouse. **B,** Representative photomicrographs of dystrophin immunostaining of the heart (Top panel, full-view images; Bottom panel, high-power images) from five AAV injected mice and an untreated DBA/2J-mdx mouse. **C,** Quantitative evaluation of AAV genome distribution in muscle and internal organs using in AAV microgene injected male DBA/2J-mdx mice (N=5). TaqMan quantitative PCR detects the junction of R1-R16. Dia, diaphragm; Gas, gastrocnemius; Quad, quadriceps; TA, tibialis anterior.

Figure S2. Micro-dystrophin expression reduces skeletal muscle disease in DBA/2J-mdx mice. A, Representative full-view photomicrographs of the HE stained quadriceps, tibialis anterior muscle (TA) and diaphragm from untreated and AAV injected DBA/2J-mdx mice. Scale bar, 500 μm. **B,** Representative high-magnification photomicrographs of the HE stained quadriceps, TA and diaphragm from untreated and AAV injected DBA/2J-mdx mice.

Figure S3. Intravenous AAV-9 delivery results in saturated micro-dystrophin expression in the extensor digitorum longus muscle in DBA/2J-mdx mice. Representative full-view photomicrographs of dystrophin immunostaining from DBA/2J. DBA/2J-mdx and treated DBA/2J-mdx mice.

Figure S4. AAV micro-dystrophin therapy improves absolute muscle force of DBA/2J-mdx mice. A, Quantitative evaluation of the absolute twitch force and absolute maximal tetanic force in the extensor digitorum longus muscle (EDL). **B,** Quantitative evaluation of the absolute twitch force and absolute maximal tetanic force in the tibialis anterior (TA) muscle. Asterisk, untreated DBA/2J-mdx mice is significant different from that of DBA/2J and AAV treated DBA/2J-mdx mice. Cross, DBA/2J is significant different from that of AAV treated DBA/2J-mdx mice.

Figure S5. DBA/2J mice show spontaneous muscle pathology. A, Representative photomicrographs of freshly dissected BL10 and DBA/2J mouse hearts. Arrow indicates epicardial calcification and/or fibrosis on the surface of the right ventricle in the DBA/2J mouse. **B,** Representative high-magnification photomicrographs of HE and Masson trichrome-stained heart sections from DBA/2J and DBA/2J-mdx mice.

Figure S6. Representative ECG and the pressure-volume loop tracing from experimental mice. A, ECG reveals the shortened PR interval in a DBA/2J-mdx mouse. Micro-dystrophin therapy did not increase the PR interval. **B,** The pressure-volume loop shows a similar hemodynamic profile in DBA/2J and DBA/2J-mdx mice.